Journal of Electrical Engineering 4 (2016) 133-149
doi: 10.17265/2328-2223/2016.03.004

Depth and Altitude Control of an AUV Using Buoyancy Control Device

Mahdi CHOYEKH[1], Naomi KATO[1], Ryan DEWANTARA[1], Hidetaka SENGA[1] and Hajime CHIBA[2]

1. Department of Naval Architecture and Ocean Engineering, Osaka University, Suita, Osaka 565-0871, Japan

2. Department of Merchant Marine, Toyama National College of Technology, Imizu, Toyama 933-0293, Japan

Abstract: A new method for depth control was developed for a spilled oil and blow out gas tracking autonomous buoy robot called SOTAB-I by adjusting its buoyancy control device. It is aimed to work for any target depth. The new method relies on buoyancy variation model with a depth that was established based on experimental data. The depth controller was verified at sea experiments in the Toyama Bay in Japan and showed good performance. The method could further be adapted to altitude control by combining the altitude data measured from bottom tracking through a progressive depth control. The method was verified at the sea experiments in Toyama in March 2016 and showed that the algorithm succeeded to bring the robot to the target altitude.

Key words: AUV, depth control, buoyancy device.

1. Introduction

Oil spills produced by accidents from oil tankers and blowouts of oil and gas from offshore platforms cause tremendous damage to the environment as well as to marine and human life [1]. To prevent oil and gas that are accidentally released from deep water from spreading and causing further damage to the environment over time, early detection and monitoring systems can be deployed to the area where underwater releases of the oil and gas first occurred. Monitoring systems can provide a rapid inspection of the area by detecting chemical substances and collecting oceanographic data necessary for enhancing the accuracy of simulation of behavior of oil and gas.

Due to their compactness, the use of AUVs for full-water surveying is being adopted increasingly [2, 3]. Among the existing types of underwater robots used to autonomously monitor marine environments in 3-D space from sea surface to seabed over the long term is the Argo Float [4] that floats vertically and repeats descending and ascending in the vertical direction by using a buoyancy control device. However, it does not have a function of active movement in the horizontal direction. Another method is the underwater glider [5], which has a streamlined body with fixed wings. It can descend and ascend also by using a buoyancy control device, while it moves in the horizontal plane like a glider for long distance. However, the ratio of vertical movement distance to horizontal movement distance is small. An AUV (autonomous underwater vehicle) called SOTAB-I (the spilled oil and gas tracking autonomous buoy system), that provides functionality that lies midway between profiling buoys and gliders, is being developed. It was designed not only to move in the vertical direction by a buoyancy control device, but also in the horizontal direction by two pairs of rotational fins. SOTAB-I can perform on-site measurements of oceanographic data as well as dissolved chemical substances using underwater mass spectrometry [6]. SOTAB-I has three main surveying modes. At the first stage, SOTAB-I performs the water column survey by adjusting its buoyancy. The rough mode is used to collect rough data on physical and chemical characteristics of plumes by repeating descending and ascending on an imaginary circular cylinder centered at the blowout position of oil and gas

Corresponding author: Mahdi CHOYEKH, Ph.D. student, research fields: naval architecture and ocean engineering.

through the variation of buoyancy and movable wings' angles. Finally, in case the UMS detects a high concentration of any particular substance, a precise guidance mode will be conducted to track and survey its detailed characteristics by repeating descending and ascending within the plume. The photograph mode enables us to have a large visual overview of the area around the blowout position of oil and gas by taking pictures of the seabed and making image mosaicking. SOTAB-I moves laterally using horizontal thrusters along diagonal lines of a polygon with a radius of 5 m centered on the blowout position of oil and gas. Therefore, the depth control is a very important task in the surveying effort which requires particular attention.

There are several methods used to control the depth of AUVs. With normal horizontal type AUVs, the depth control is performed by horizontal wings. For the vertical type AUVs, a buoyancy control device is normally used for depth control. There exist a variety of mechanisms to adjust the buoyancy. In the submarines for example, the amount of the air/seawater of trim or ballast tanks is controlled to adjust the buoyancy. When the submarine is on the surface, air is filled in the ballast and the submarine becomes positively buoyant. To start diving, water is introduced into the ballast tanks while the air is vented outside until it becomes negatively buoyant leading the submarine to sink. Compressed air is stored in flasks to adjust the amount of water inside the ballast tank during operation. Another widely employed mechanism in AUVs is to adjust the volume of the robot through a device that compresses and expands the air contained in a cylinder. This mechanism is characterized by its reliability and its relative fast response. However, the motor pump, used to ensure the compression and the expansion of the air, generates noise. Additionally, when the robot is decreasing its buoyancy, an amount of the ballast water (seawater) is pulled from one region and then, may be dumped in another region to increase buoyancy. This represents a risk of dumping living organisms in an environment different from their original inhabiting region, which may harm their new environment. This problem is referred as the ballast water problem [7, 8]. Among other existing technologies, there is the metal bellow mechanism, which imitates the change of state of the spermaceti oil from liquid to solid and vice versa, leading to change of density, in the sperm whale [9]. Similarly, AUV using metal bellow mechanism relies on the change of state of a low melting point liquid, such as wax [10] or oil [11], by adjusting its temperature. This mechanism does not make noise and presents an ecological advantage over other systems since it does not involve any discharging of ballast materials, eliminating the ballast water problem. However, results show that their response time is slow and is energetically costly since the temperature of the oil should be maintained. A third mechanism imitates ray-finned fish, which adjust the volume of their bladders to adjust their buoyancy [12]. They employ polymer buoyancy control device [13]. Electrolysis is used to generate pure hydrogen, which is a clean gas, in order to expand the volume of an artificial bladder leading to a displacement of water and an increase of buoyancy. To reduce the robot buoyancy, extra amount of gases are simply released outside via a valve. These systems are characterized by their silent operation. However, they are more oriented for small devices operating near the sea surface where the water pressure is not significant. Due to the reliability and the fast response as well as their low power consumption, the buoyancy variation through the adjustment of the air volume in a cylinder mechanism was employed. The ballast water problem does not apply for SOTAB-I since it is designed to operate around the same region of the blow out gas. The noise caused by the motor pump may be reduced by choosing a high quality actuator.

For the same control mechanism, there exist several control strategies. An implementation of a cascaded velocity-position PID controller was used in a coastal profiling float by Ref. [14]. The method consists of

adjusting the velocity set point according to depth error between the current and target depths. The vertical velocity is controlled through a PID controller to achieve the desired depth. The algorithm succeeded to achieve the desired depth near the sea surface, but at a high energy cost. Another control strategy is employed in the underwater gliders where the buoyancy control device is performed simultaneously with a mechanism of gravity center movement in horizontal plane. On the other hand, Argo float uses only buoyancy device to adjust their depth. To do so, the float relies on the establishment of a highly accurate ballasting curve [15]. This requires a high precision ballasting experiment to adjust the robot's density in a way to become equal to the density of the seawater, which will be measured by a highly accurate CTD sensor, at the designated parking depth. This will lead the robot to reach its neutral buoyancy point.

There are many challenges and constraints associated with depth control of underwater vehicle. For instance, at-sea experiments require enormous financial and logistic resources limiting the experiments time. Hence, it is important that the program should be easy to implement and repeatedly verified by simulating programs before its real deployment. On the other hand, environmental constraints like a considerable variation of the density of water between the sea surface and the seabed bring complications in the control because they lead to the variation of the neutral buoyancy value of the robot. Even if the neutral buoyancy of the robot is determined accurately at a certain spatial condition, there is no guarantee that the robot will keep its vertical position due to the up-welling and down-welling water currents. Other constraints are represented by the hardware limitations. In fact, the buoyancy device employed has three controlling states: it can be controlled to increase the buoyancy, decrease it or stay idle. However, it is not possible to change the rate of variation directly. In addition, the rate of change of buoyancy is relatively slow, not symmetric in both directions and varies with depth. Moreover, the change of the buoyancy variation orientation is not instantaneous, there is a lag time of 2 s between each change of state. The oil level sensor has also an inaccuracy within ±0.1%. Previously, a PID controller was developed for depth control [16]. It gave good performances and small overshoot, but only for a depth range up to 100 m. Beyond that limit, significant overshoot was reported. The previous controller relied on a very accurate determination of the neutral buoyancy. In addition, the PID control parameters were not adaptive. Besides, it does not enable to freeze the robot at the target depth. For the lacks mentioned before, it is necessary to develop a new controller that overcomes the shortening and take in consideration the environmental and hardware constraints. A new method for depth control was developed. It is aimed to work for any target depth and to freeze the robot at the target depth. The method relies mainly on the buoyancy variation model with depth established based on tank and at-sea experimental data. The paper is organized as follows: Section 2 gives an overview of SOTAB-I hardware and its buoyancy device. Section 3 studies the buoyancy variation at tank and sea experiments and establishes its model. Section 4 and 5 deal, respectively, with the depth control and the altitude control algorithms and the experimental results obtained of their execution in Toyama Bay experiments in March 2016. The final section gives the conclusions of the work.

2. SOTAB-I Overview and Hardware Description

2.1 Outlines of SOTAB-I

The SOTAB-I is 2.5 m long and weighs 325 kg. It can be submerged in water as deep as 2,000 m. It is able to descend and ascend by adjusting its buoyancy using a buoyancy control device while changing its orientation through two pairs of movable wings. The SOTAB-I can also move in horizontal and vertical directions using two pairs of horizontal and vertical thrusters. A visual overview of SOTAB-I is illustrated

in Fig. 1, and its main characteristics are summarized in Table 1. The arrangement of devices and sensors installed on SOTAB-I is shown in Fig. 2.

When the robot floats on the sea surface, a WLAN (wireless local area network) and an iridium satellite communication transceiver module are used for data transmission. When the robot is underwater, the user on the mothership and the SOTAB-I can communicate through the acoustic modem.

The robot tracking on the sea surface is ensured by a GPS (global positioning system) receiver that serves to determine the robot's absolute position. In the case where the robot is submerged, tracking is ensured by the USBL (ultra-short baseline) system. The vertical position of the robot in the water column is given by depth data from the CTD sensor. When the robot is within the bottom tracking altitude from the seabed, the DVL (Doppler velocity logger) is able to measure robot's velocities. The robot motion and orientation are given by the compass and the IMU (inertial measurement unit).

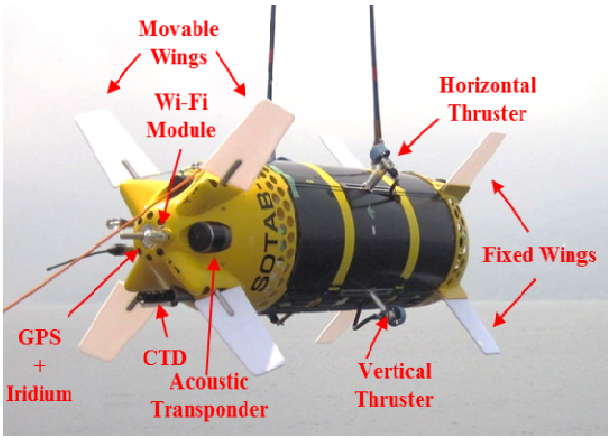

Fig. 1 SOTAB-I robot.

Table 1 Principal particulars of SOTAB-I.

Total length [mm]	2,503
Diameter [mm]	667
Weight in air [kg]	311.7
Weight in water [kg]	± 3.8

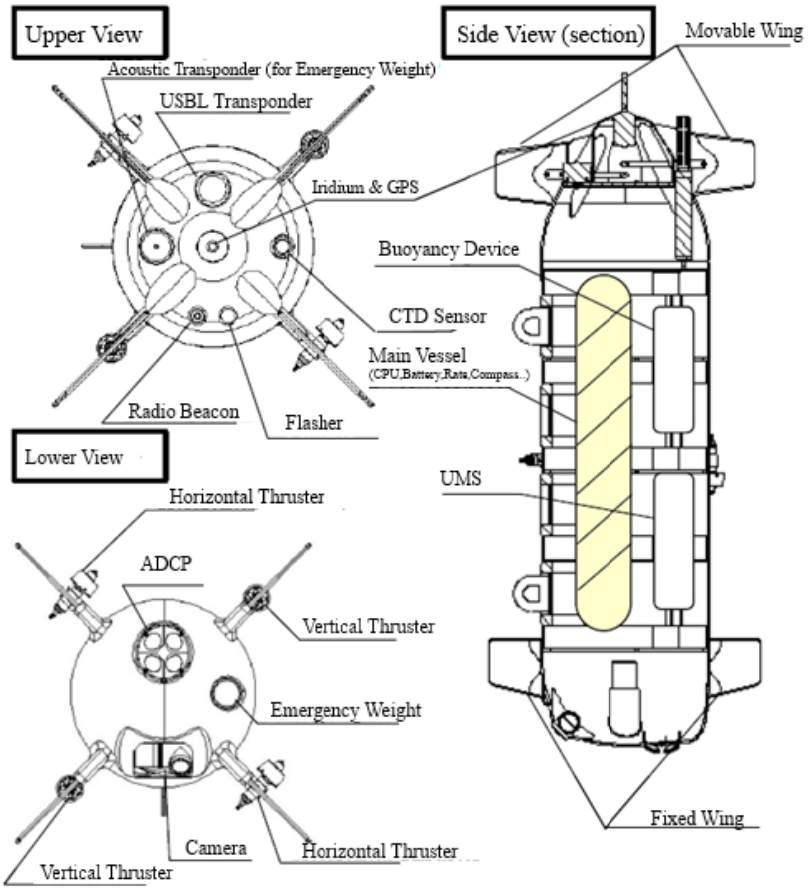

Fig. 2 Arrangement of devices and sensors installed on SOTAB-I.

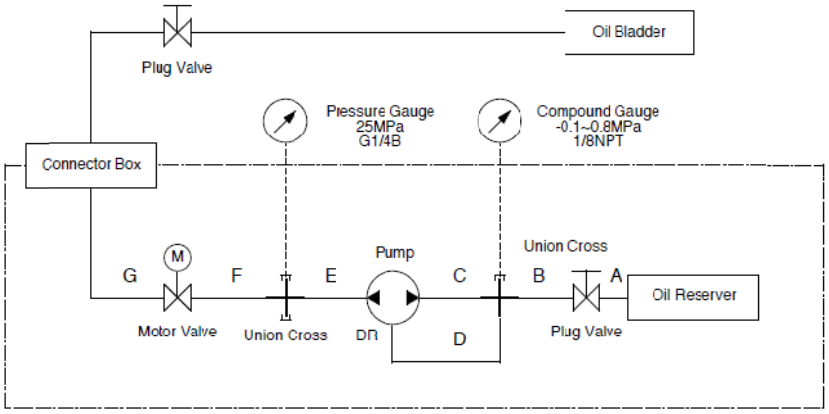

Fig. 3 Buoyancy device.

An ADCP is employed to measure the magnitude and orientation of water current layers. SOTAB-I is also fitted with a UMS to determine the characteristics and physical properties of the dissolved gas and oil. To obtain a visual representation of blowouts of plumes of gas on the seabed, the robot is equipped with a camera.

2.2 Buoyancy Device

In the buoyancy control device, an oil hydraulic pump injects and extracts oil between the external oil bladder and the internal oil reservoir. A motor valve serves to automate opening and closing cycles, and a brake is used to lock the pump (Fig. 3). The flow rate during the injection of oil into the bladder at the external pressure of 20 MPa is 243 mL/min, and during the extraction of oil from the bladder at the same external pressure condition, it is 349 mL/min. In total, six digital inputs are employed to control the buoyancy device. A digital input serves to control the power supply relay. One input is used to open the valve and another to close it. To control the motor pump actuator, one input is used to run/disable it and another one specifies the rotation direction. One more serves to activate/deactivate the brake. The feedback is provided by two digital outputs that report the valve position, and one analog output that provides the oil level.

Fig. 4 depicts the relationship between the pressure in the reservoir and the volume of the oil in the reservoir. The “pressure in the reservoir” is the pressure applied by the hydraulic pump to the oil reservoir cylinder. The maximum allowable drain pressure of the pump is 0.03 MPa. The oil reservoir is fitted with a linear potentiometer whose analog output voltage is an image of the piston displacement under the pump drain pressure. The voltage is proportional to the oil volume of the reservoir, which leads to the variation of robot buoyancy, as shown in Table 2. When the oil room is full, the output voltage is 0.3892 V. When the oil room is empty, the output voltage is 1.6208 V. Because the reservoir has a cylindrical shape and the surface of the base is constant, the output voltage of the potentiometer can be used to determine the volume of the oil in the reservoir, which explains the linear volume/output voltage relationship. The mass change can be obtained after multiplying the volume change with the density of seawater, which is typically equal to 1,024 kg/m^3.

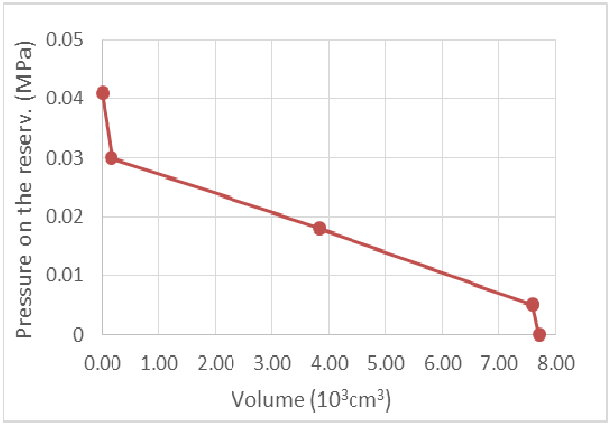

Fig. 4 Relationship between the pressure and the volume in the oil reservoir.

Table 2 Variation of robot buoyancy against voltage on motor.

Mass change (seawater) (g)	Volume change (cm^3)	Potentiometer output voltage (V)	Pressure (MPa)
7,884.8	7,700.0	1.621	0
7,746.6	7,565.0	1.599	0
7,763.2	7,581.2	1.602	0.005
3,925.7	3,833.7	1.012	0.018
171.8	167.8	0.443	0.030
0	0	0.389	0.041

3. Establishment of the Buoyancy Model

The objective in this section is to establish a time model and a buoyancy model. The time model is needed for the depth control of the robot. It enables to estimate the time needed for SOTAB-I to change its buoyancy from its current value to a target value. The buoyancy model is also needed for the simulating program. It enables to estimate the variation of the buoyancy value from its initial value every sampling period. We consider establishing a model for the buoyancy variation from 20 to 85% up to 1,000 m water depth based on the experiments results obtained at pressure tank and at-sea.

3.1 Experiments Results of Buoyancy Variation

3.1.1 Pressure Tank Experiments

Pressure tank experiments were performed to calculate the time necessary for changing 7,500 cc of oil in the reservoir in both directions. OUT->IN direction is when the oil hydraulic pump injects and extracts oil from the external oil bladder and injects it to the internal oil reservoir. IN->OUT is the opposite direction.

Based on Fig. 5 and Table 3, the time needed to change the buoyancy corresponding to 7,500 cc in the OUT>IN direction is constant till 10 MPa (~1,000 m water depth). From 10 MPa to 20 Mpa, it can be modeled as a linear function. The time difference between the full scale variation of buoyancy at 0 MPa and 20 MPa is less than 9 minutes. For the IN>OUT direction, the buoyancy variation time is almost same from 0 up to 10 MPa. Beyond that limit, it becomes slightly faster.

3.1.2 At-sea Experiments

Fig. 6a confirms the results obtained in the pressure tank. The buoyancy variation rate is almost same from 0 to 100 m. Hence, the time and buoyancy models in the OUT>IN direction can be modeled as a linear function. Fig. 6b dates from an experiment on the 20th of March 2015 in Toyama Bay. It shows the buoyancy variation in the IN>OUT direction from 20 to 85% at 1 m and 700 m water depths. It shows that buoyancy variation can be represented under the form of a 3rd degree polynomial function as shown in Table 4.

3.2 Model of the Buoyancy Variation with Depth

Based on the experimental data, the buoyancy variation in the OUT>IN direction can be modeled as a linear function.

$$T_c \text{ (OUT->IN)} = -15.122 * (B_t - B) \quad (1)$$

In the IN>OUT direction, the main parameter that

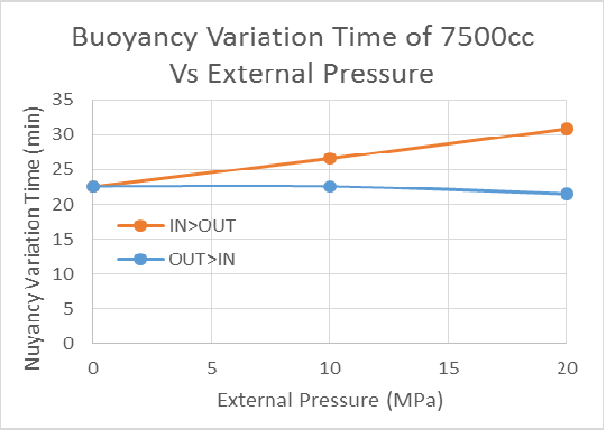

Fig. 5 Relationship between the pressure and the buoyancy variation time.

Table 3 Time of variation of robot buoyancy with pressure.

	External pressure	Motor rotation speed	Flow rate	Time
	MPa	rpm	cc/min	min/7,500 cc
IN>OUT	0	7,865	331	22.6
	10	6,700	282	26.6
	20	5,760	243	30.9
OUT>IN	0	7,865	331	22.6
	10	7,865	331	22.6
	20	8,300	349	21.5

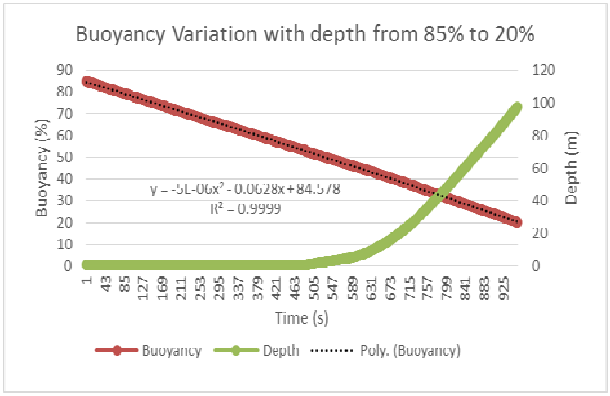

(a) OUT>IN

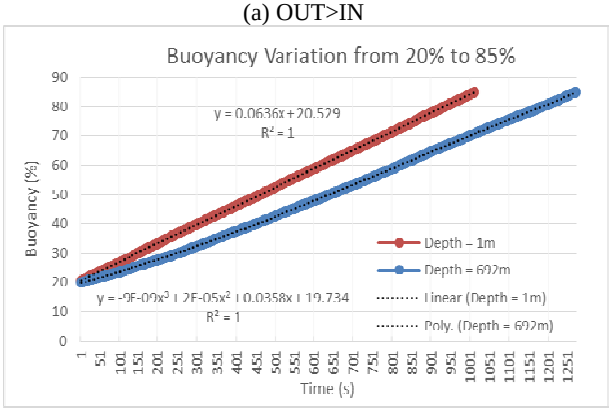

(b) IN>OUT

Fig. 6 Buoyancy variation with depth on 20th March 2015 experiment.

Table 4 Buoyancy variation model of 20th March 2015 experiment.

Direction	Depth	Buoyancy variation
OUT>IN	1 to 700 m	$T_c = -15.122 * (B_t - B)$
IN>OUT	1 m	$T_c = 15.122 * (B_t - B)$
	700 m	$T_c = 0.0015 * (B_t^3 - B^3) - 0.2688 * (B_t^2 - B^2) + 34.065 * (B_t - B)$

contributes considerably in the change of the buoyancy variation speed is the depth. The model can be generalized and written under the form of 3rd degree polynomial function that depends on the depth D.

$$T_c\ (IN->OUT) = C_3(D) * (B_t^3 - B^3) - C_2(D) * (B_t^2 - B^2) + C_1(D) * (B_t - B) \quad (2)$$

Linear interpolation and extrapolation of the coefficients a, b and c are used to determine the buoyancy model at a certain depth based on the models established for depths equal to 1m and 700m. The following equation shows the formula used to calculate C_i (D) for i = {1, 2, 3}

$$C_i\ (D) = (C_i\ (1) - C_i\ (700)) * D / (700 - 1) \quad (3)$$

Knowing that

At 700 m $C_3 = 0.0015$; $C_2 = 0.2688$; $C_1 = 34.065$

At 1 m $C_3 = 0$; $C_2 = 0$; $C_1 = 15.122$.

3.3 Comparison between Buoyancy Variation Model and Experimental Data

Data of buoyancy variation time in several ranges were collected from previous at-sea experiments of SOTAB-I and compared to the values obtained by the model. To estimate the accuracy of the model, we defined the ratio Time/Range to estimate the time deviation of the model in seconds for every 1% of buoyancy variation. Table 5 summarizes the obtained results.

Table 5 shows the estimated time of buoyancy variation is close to the values obtained from experiments. The maximum deviation was obtained when the buoyancy variation is between 20% and 30%. The time estimation in the OUT>IN direction does not exceed 0.5 s per 1% of buoyancy variation at full range, suggesting a high accuracy of the model in that direction. On the other hand, in the IN->OUT direction, the maximum values of deviations were obtained in the

Table 5 Comparison between the buoyancy variation model and experimental results.

Experiment	Depth	Orientation	Range of variation	Tc (experiment)	Tc (model)	Time/range (s/1%)
5/25/2015 2:28:43	Air	OUT>IN	95%→21%	1,121 s	1,119 s	–0.03
		IN>OUT	20%→94%	1,166 s	1,164 s	–0.03
11/27/2014 9:20:56	0~95 m	OUT>IN	79%→20%	859 s	892 s (50 m)	+0.56
	700 m	IN>OUT	20%→85%	1,274 s	1,340 s (700 m)	+1.01
11/28/2014 9:48:23	0~42 m	OUT>IN	78%→31%	703 s	710s	+0.15
	0~100 m	IN>OUT	31%→79%	854 s	823 s (50 m)	–0.65
3/20/2015 14:12:33	95~155 m	IN>OUT	20%→30%	178 s	199 s (155 m) 184 s (95 m)	+2.1 +0.6
	155~198 m	IN>OUT	30%→40%	176 s	192 s (155 m) 193 s (198 m)	+1.6 +1.5
	198~210 m	IN>OUT	40%→49%	170 s	169 s (198 m)	–0.11

20 to 30% range, but did not exceed 2.1 s per 1% variation of buoyancy. So we can consider the overall model as reliable. It is important here to mention that the model accuracy can be improved by feeding the model with additional experiment data at various depths which will reduce the model interpolation and extrapolation error.

4. Depth Control

4.1 Control Algorithm

Depending on the operating mode, there are two main scenarios to be considered. The first is that the robot reaches the target depth and subsequently starts ascending, like in the rough mode. The second is to bring the robot to the target depth and freeze it there until an ascending order is received through acoustic communication or ascending timer overflow. Therefore, we can decompose the control program into two main steps. As shown in Fig. 7, the first step is to bring the robot from its current depth (D) to a set target depth (D_t) using a predictive depth controller. Once the target depth is reached, the second step is executed to stabilize it around the target depth.

In the next part we explain in details the predictive controller and the depth stabilization algorithm.

4.1.1 Predictive Control

As shown in Fig. 8, we introduce the configuration parameters of the program at the beginning of the experiment. For instance, the estimated value of the neutral buoyancy (B_n) with the margin of uncertainty around it (B_m). We also input the value of sensors random error of the oil sensor (B_{err}) and of the depth data (D_{err}) of the CTD sensor, based on the sensors' data collected in the previous experiments.

Once the program m is executed and its configuration is over, the predictive controller is executed every second. At first the robot updates all the sensors' data, such as the depth (D), provided by the CTD sensor, and the value of the current buoyancy (B), measured by a linear potentiometer image of the oil level. Other data can be derived based on the raw data, such as the vertical speed (S).

Fig. 9 shows the predictive control inputs and outputs diagram and Table 6 defines all the parameters related to the predictive controller.

At every second, it is possible to have an estimation of the time needed to reach the target depth (T_r) using Eq. (4).

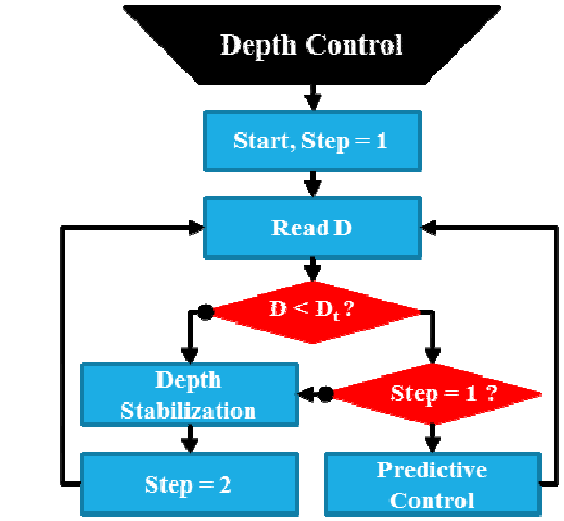

Fig. 7 Depth control process.

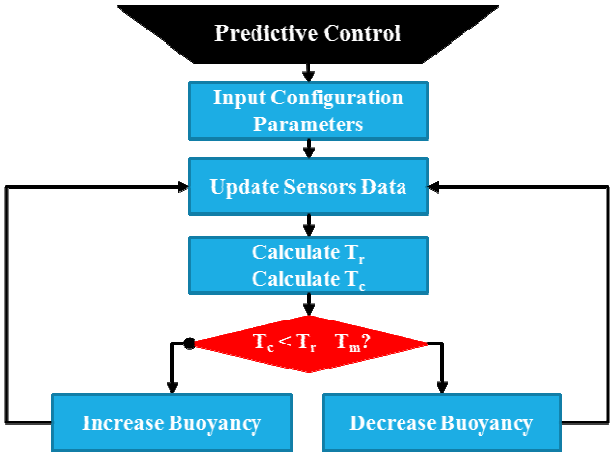

Fig. 8 Predictive depth control flowchart.

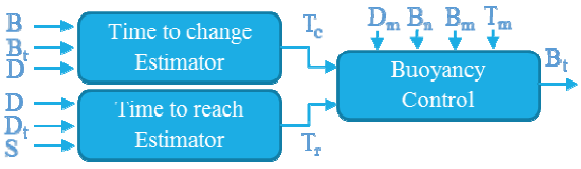

Fig. 9 Predictive depth control input/output diagram.

Table 6 Definition of the buoyancy control parameters.

Symbol	Definition
D	Current depth (m). D > 0
D_t	Target depth (m)
D_m	Margin of tolerance around D_t
S	Current speed (m/s). S > 0 ➔ Robot descending
S_m	Speed margin
B	Current buoyancy (%). Range: 20->95%
B_t	Output target buoyancy
B_n	Neutral buoyancy
B_m	Margin of tolerance around the neutral buoyancy B_n
T_c	Time needed to change the buoyancy from B to B_t in (s)
T_r	Time needed to reach the target depth based on the current speed of the robot
T_m	Time margin used for security purpose. It compensates eventual inaccuracy in the buoyancy model

$$T_r = ((D_t - D) / S) \quad (4)$$

The buoyancy variation model, established in the previous section of this paper, enables to estimate the time (T_c) needed for changing the robot buoyancy from its current value to the neutral buoyancy. The first step is based on the continuous estimation of the time to reach (T_r) and the time to change (T_c) while decreasing the buoyancy value, till the stop condition is reached. We introduce Tm, which corresponds to the time error margin used to compensate eventual inaccuracies in the buoyancy device model.

If the estimation of $T_r > T_c + T_m$ it means that it is possible to increase the vertical speed of the robot since we have enough time to change the buoyancy to its neutral level. Hence, we decrease the target buoyancy value.

In the case where $T_r <= T_c + T_m$, then it means we have just enough time to change the buoyancy to the neutral level before the robot reaches its target depth. Hence, we start to increase the buoyancy of the robot progressively.

4.1.2 Depth Stabilization

Several algorithms can be used for depth stabilization. Among the most used are the PID controllers. However, one of the drawbacks of these controllers is that they require the actuators to operate at full time, which increases the power consumption. In addition, in our robot's case, the buoyancy variation speed is not constant and varies with depth. Furthermore, its variation is not symmetric in both IN->OUT and OUT->IN directions. For that reason, a conventional PID controller is not suitable, which requires the development of an asymmetric PID controller that adapts its parameters with the robot's depth. This will add a lot of complexity to the program and requires a longer time to implement it and to validate its performance. For that reason, we chose to use a heuristic controller for depth stabilization. The latter provides a simple way to control the depth. It is based on heuristic rules that enable to adjust the buoyancy based on the current depth and vertical speed of the robot. If we take the case where the robot depth (D) is below the target depth (D_t), we can establish the following rules, to be executed by priority order:

- If the robot is below the maximum tolerated depth ($D_t + D_m$), then increase the buoyancy;
- If the robot is below D_t and it is descending, then increase buoyancy;
- If the robot is below Dt, but it is ascending fast above a speed margin (S_m), then decrease buoyancy;
- If the robot is below the target depth, and it's ascending slowly below (S_m), then the buoyancy actuator is idle.

Fig. 10 shows the flowchart of all the algorithm. It is important to mention here that the buoyancy variation values are limited between $B_n + B_m$ and $B_n - B_m$.

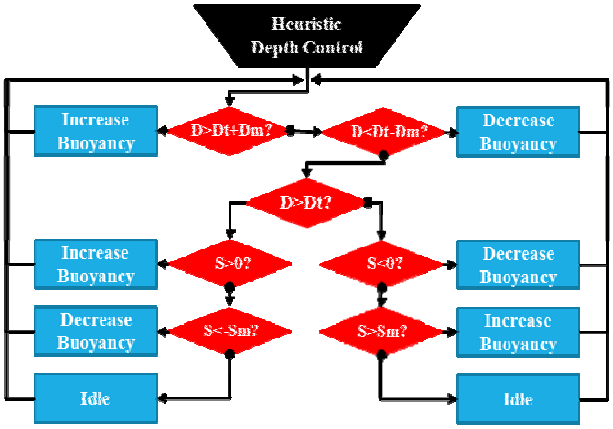

Fig. 10 Heuristic control flowchart.

Table 7 Parameter configuration.

General parameters	Value
Target depth (D_t)	500 m
Neutral buoyancy (B_n)	62.5%
Buoyancy margin (B_m)	2.0%
Buoyancy control threshold (B_{diff})	0.2%
Buoyancy device accuracy (B_{err})	0.05%
Predictive control parameters	**Value**
Time margin (T_m)	20 s
Depth margin (D_m)	0.5 m
Depth stabilization parameters	Value
Vertical speed threshold (S_m)	0.02 m/s
Depth threshold	5 m
Stabilization period	900 s

4.2 Experiments Results

The depth control experiment was conducted in Toyama Bay on 17th March 2016. The robot was ordered to reach a set target depth equal to 500 m and stay there for 15 minutes before ascending to the sea surface. Hence, the control program can be divided into 3 main steps: In the first step, the robot uses the predictive depth control to reach the target depth (Step 1). Then the depth stabilization algorithm using the heuristic control is executed to freeze the robot depth for 15 minutes (Step 2). Finally, the target buoyancy is set to its maximum value to bring the robot to the sea surface (Step 3). For that purpose, the depth control parameters were configured as shown in Table 7.

Fig. 11 shows the result of the experiment. As it can be observed, the robot managed to reach the target depth and freeze there for 15 minutes before starting the ascent.

Fig. 12a shows the variation of the robot's vertical speed with depth under the effect of the buoyancy

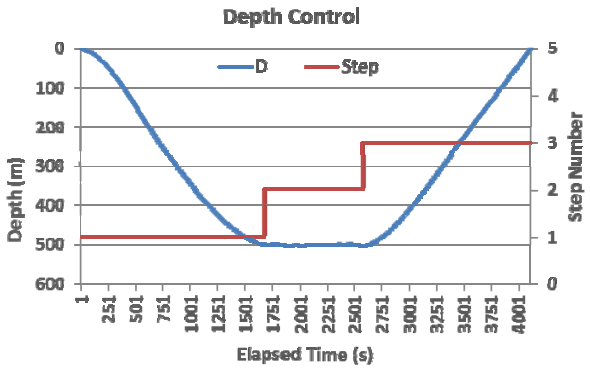

Fig. 11 Depth control.

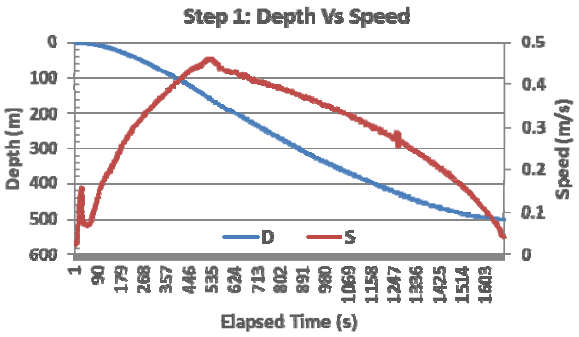

(a) Depth Vs Speed

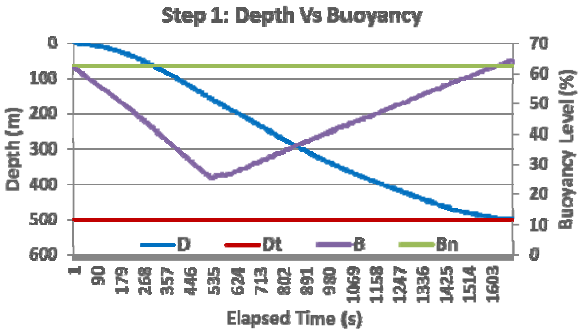

(b) Depth Vs Buoyancy

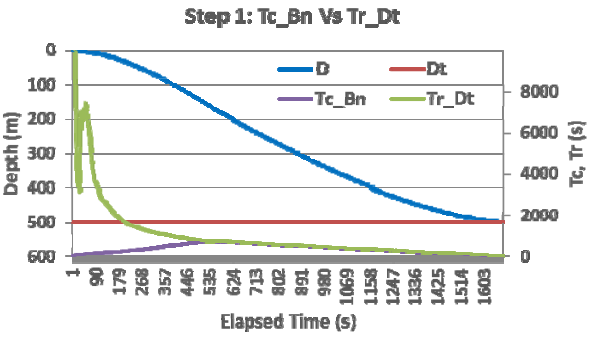

(c) T_c Vs T_r

Fig. 12 Predictive depth control.

control shown in Fig. 12b. The time to reach the target depth (T_rD_t) and the time needed to change to the neutral buoyancy (T_cB_n) are shown in Fig. 12c. The latter parameters define whether the buoyancy should be increased or decreased as explained in the flowchart in Fig. 7. It can be observed that robot managed to reach the target depth with a vertical speed near 0 m/s at a buoyancy value near the neutral. The control algorithm succeeded to balance the robot's vertical speed based on the compromise between T_cB_n and T_rD_t.

Fig. 13 shows the result of the depth stabilization algorithm. It shows that the control program maintained the robot speed within the interval of tolerance around the target depth equal to 5 m. In addition, the control program succeeded to limit the robot's vertical speed to less than 5 cm/s (check Sm threshold).

In addition, though the real neutral buoyancy was 64% and not 62.5% as set in the program, the control program succeeded in controlling the robot at the set depth.

Fig. 14 shows the robot's ascent. The maximum speed was equal to 0.4 m/s. The sudden variation of the vertical speed is due to the change of the wings' angles.

As a conclusion, the predictive control program succeeded to bring the robot to the target depth without overshoot at a buoyancy value equal to the neutral and a vertical speed close to 0. On the other hand, the depth stabilization algorithm managed to keep the robot near the target depth at a limited overshoot and a very small vertical speed. Furthermore, the control program proved its robustness: Though the estimated neutral buoyancy was slightly different from the real neutral buoyancy, the robot managed to reach the exact target depth without problem.

5. Altitude Control

There are several operating modes that require SOTAB-I to get close to the seabed. For example in the photograph mode, SOTAB-I needs to approach the seabed to be able to take neat pictures of the blow out position. Similarly, in the water column measurement

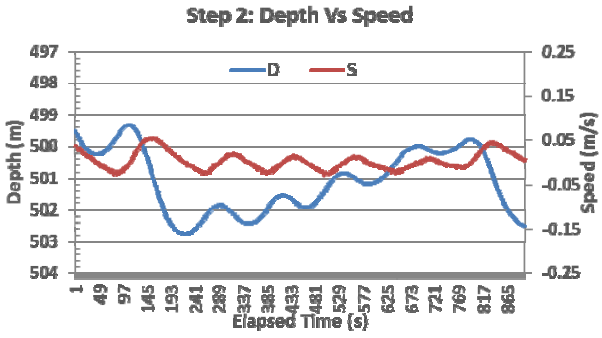

(a) Depth Vs Speed

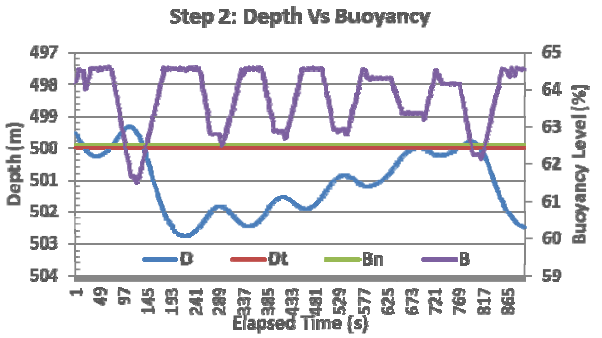

(b) Depth Vs Buoyancy

Fig. 13 Depth stabilization.

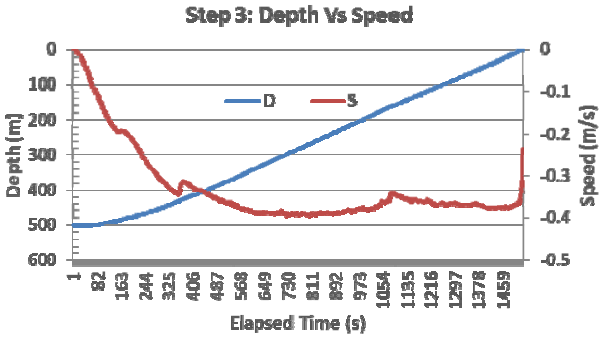

(a) Depth Vs Speed

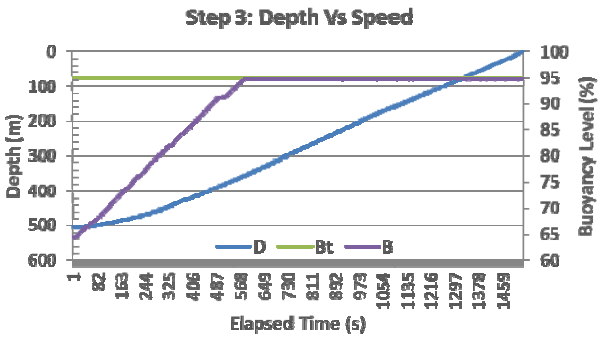

(b) Depth Vs Buoyancy

Fig. 14 Robot's ascent.

mode, the robot is required to dive from the sea surface to near the sea bed to obtain a full water column profile. Hence, it is important to develop a program that controls the altitude of the robot. One way is to use the vertical thrusters to control the altitude. However, there is a risk that they mix up the sediments on the seabed which influences the transparency of the water. In addition, they will disturb the water flow, causing some inaccuracies in the water current measurement. To overcome the previously mentioned weaknesses, we suggest a second method that only uses the buoyancy device as an actuator to control the altitude of the robot.

5.1 Control Algorithm

The method consists of the adaptation of the depth control algorithm detailed in the previous section to altitude control. It is important to remind here that the robot is only able to measure the altitude from the seabed when the bottom tracking is active. Hence, the set target altitude should be within bottom tracking range.

Fig. 15 illustrates the flow chart of the altitude control algorithm. It consists of 3 stages of predictive depth control followed by an altitude stabilization control executed to keep the robot at the set target altitude.

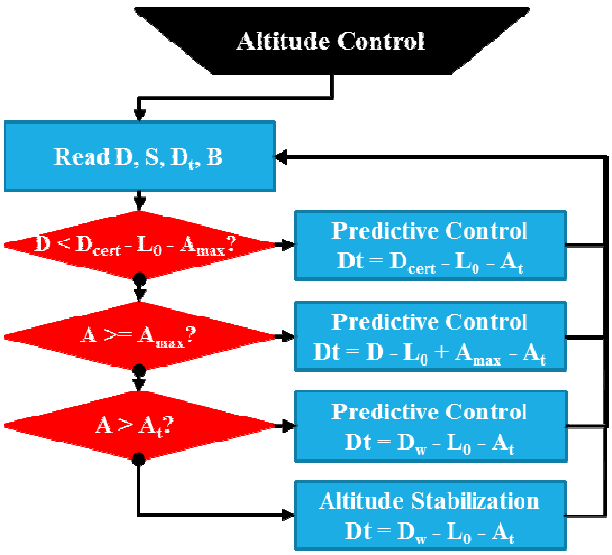

Fig. 15 Altitude control flowchart.

If we consider the case where the water depth is unknown, then there is a possibility that the robot gets close to the seabed at any moment. Hence, to ensure that the robot can stop descending the buoyancy should be set near the neutral buoyancy value in a way to guarantee that the robot will be able to reach the neutral buoyancy on time. This has a direct impact on the robot speed which becomes very slow and then extends the experiment time and its cost. However, in real experiments, it is possible to get a rough estimate of the water depth from the GPS position. The determination of a safe approximation of the water depth contributes considerably to the reduction of the time needed to reach the target altitude.

Following are the altitude control steps:

Step 1: The robot dives with a fast speed until the depth of the robot reaches the depth limit (D_{cert}) of the "Certain depth". The "Certain depth" is the certain minimum water depth value. D_{cert} is input by the user on board before starting the descent. In this first step, the depth control with time estimation scheme is used. At first, the buoyancy control device will decrease the buoyancy. After the buoyancy level becomes lower than the neutral buoyancy of the robot, SOTAB-I will start diving. The buoyancy control device will continue to reduce its buoyancy level down up to 20%, which is set as the minimum buoyancy level of the buoyancy control device, with maximum speed. Then it will increase again its buoyancy level close to the neutral buoyancy level. The purpose of this strategy is that the robot should have enough time to change its buoyancy level to its neutral buoyancy when reaching the target depth. In this step, the target depth (D_t) is set at a fixed value as shown in the following equation:

$$D_t = D_{cert} - L_0 - A_t \quad (5)$$

where $L_0 = 2.04$ m is the distance between the CTD and the DVL sensors, A_t is the target altitude.

Step 2: When the robot is near the certain depth limit, the variable target depth control is started. D_t is calculated as follows:

$$D_t = D_{Cert} - L_0 + A_{max} - A_t \quad (6)$$

After passing the certain zone limit, there is a chance that the DVL will detect the seabed and output its current altitude (A). Therefore, the buoyancy change is limited up to the time (T_r) needed to reach the target depth. In this step, the depth control with time estimation is still being used. However, the target depth (D_t) is set equal to the current depth (D) plus the DVL range A_{max} minus the target altitude (A_t). The target depth will continuously change as the depth D of the robot decreases. Hence, it is a depth control with variable target depth. At this point, the buoyancy level of SOTAB-I is already close to the neutral buoyancy. Therefore, there will not be much change in the buoyancy level to ensure that the robot is able to stop when reaching the target depth, as shown in step 2. As a result, the robot will dive at a steady speed.

Step 3: When the DVL detects the seabed, the sea water depth (D_w) can be calculated as the sum of the depth D measured by CTD and the altitude (A) measured by DVL taking in consideration the distance (L_0) between the two sensors as shown next.

$$D_w = D + L_0 + A \quad (7)$$

Once the water depth is known, it becomes possible to transform the altitude control to an equivalent depth control using the following equation:

$$D_t = D_w - L_0 - A_t \quad (8)$$

The water depth D_w is defined as the sum of the depth D measured by CTD and the altitude A measured by DVL. This step is also carried out by using the depth control with time estimation scheme.

Step 4: When the robot is within the range of the target depth plus or minus the depth margin D_m, the depth control method is switched from the depth control with time estimation to depth stabilization control program. The depth margin D_m is usually set around 1 m as a compensation in the control mechanism of the buoyancy device. SOTAB-I will stay within the target depth for a certain period of time, which has been set on the timer. When the timer reaches zero, the robot will start ascending.

5.2 Experiments Results

In this experiment, the robot was ordered to go to a target altitude equal to 9 m then freeze there for 5 minutes before ascending to the sea-surface. The exact water depth at the place where the robot was launched was unknown, but the water depth was estimated to be at least equal to 724 m. The parameters of the altitude control were set as shown in Table 8.

Fig. 16 shows the experiment result of the altitude control. It can be observed that the robot managed to reach near the seabed and freeze there for 5 minutes before ascending.

From the DVL data, we could measure the water depth which was equal to 766 m. The control algorithm was composed of 5 steps. The first four steps were explained in Section 1. The fifth step corresponds to the robot ascent.

Fig. 17 illustrates the details of the predictive depth

Table 8 Altitude control parameters configuration.

Certain depth	724 m
Target Alt.	9 m
Ascending timer	300 s
BT min range	24
D_m	0.5 m
D_{err}	0.007 m
S_m	0.02 m/s
B_n	62.5%
B_m	2%
B_{diff}	0.2%
B_{err}	0.05%
T_m	20 s

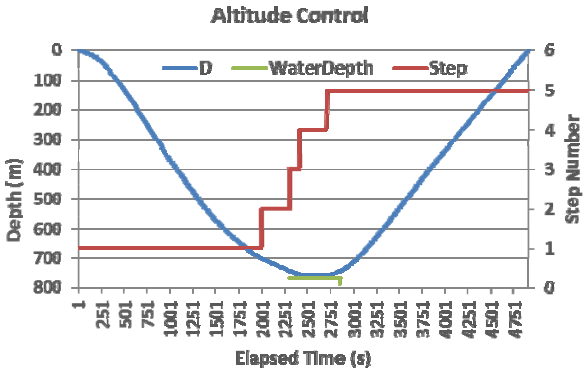

Fig. 16 Altitude control.

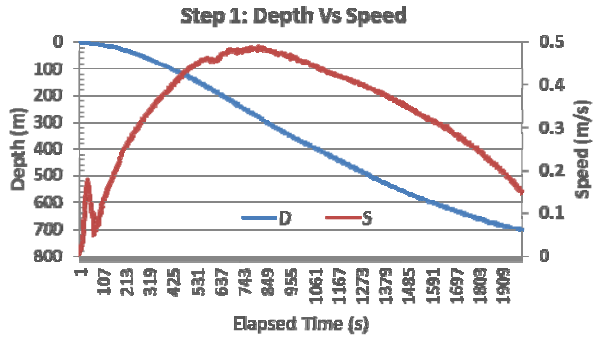

(a) Depth Vs Speed

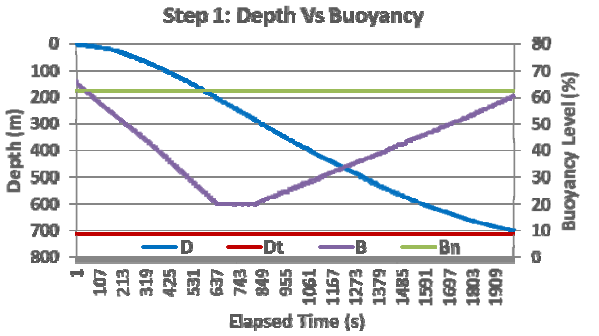

(b) Depth Vs Buoyancy

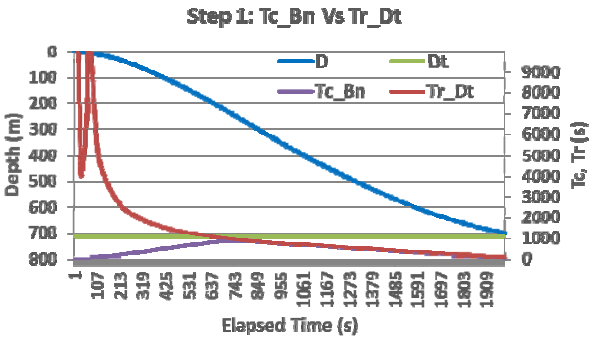

(c) Tc Vs Tr

Fig. 17 Altitude control: Step 1.

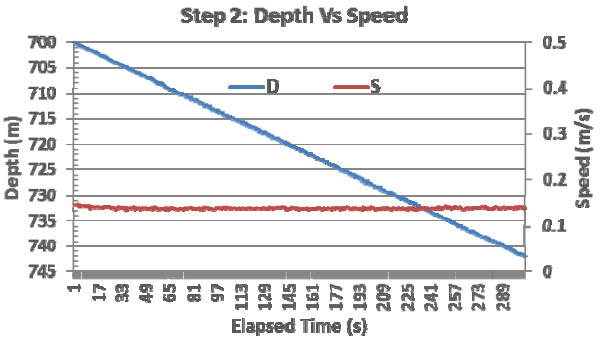

(a) Depth Vs Speed

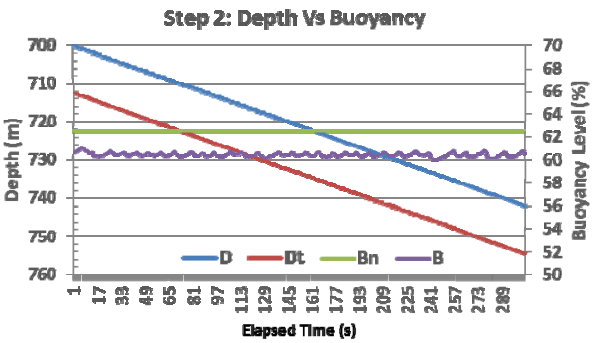

(b) Depth Vs Buoyancy

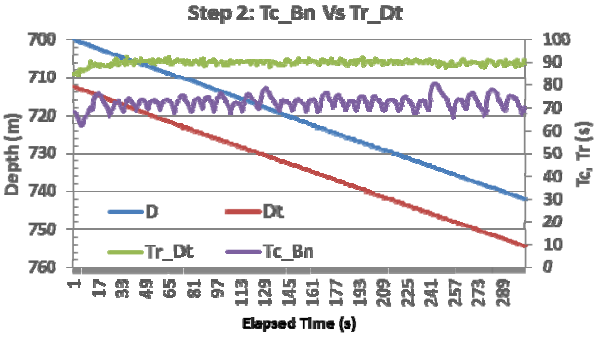

(c) Tc Vs Tr

Fig. 18 Altitude control: Step 2.

control applied in step 1 with a set target depth equal to 713 m, which can be calculated using Eq. (10) knowing that the certain depth is defined as equal to 724 m and the target altitude is equal to 9 m. It can be observed that the robot reached the minimum buoyancy equal to 20% at a maximum vertical speed equal to 0.49 m/s and maintained it for 175 s, which enabled to reduce the time of the experiment. At the end of step 1, the robot's vertical speed was reduced to less than 0.15 m/s and the buoyancy was equal to 61%, which is 3.5% below the maximum value of the estimated neutral buoyancy ($B_{n\_Max} = B_n + B_m = 62.5\% + 2\% = 64.5\%$).

At that buoyancy value, the buoyancy device is able to change to reach the neutral buoyancy on time in case the robot detects the seabed.

Fig. 18 illustrates the results of the predictive control with variable target depth. At this step, since the robot did not detect the seabed, it descends slowly in a way to be sure that the robot will be able to stop at the target altitude. In this step, the robot buoyancy is almost constant. As a consequence, the robot speed is also constant and equal to 0.14 m/s.

At 742 m water depth, the robot detected the seabed and the 3rd step was activated. The target altitude was

transformed to an equivalent target depth D_t = 755 m. As shown in Fig. 19, the predictive depth control program succeeded to smoothly reach the robot at the target depth with a vertical speed almost equal to 0 and a value of buoyancy very close to the neutral buoyancy.

To freeze the robot at the target altitude, a depth stabilizer algorithm is used. The result of its implementation is shown in Fig. 20. It shows that the robot succeeded to keep its depth within (+/-) 1 m from set target depth.

Fig. 21 illustrates the robot ascent to the sea surface. The maximum speed reached was 0.39 m/s.

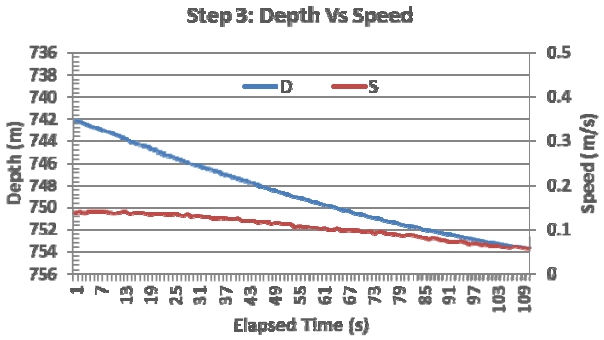

(a) Depth Vs Speed

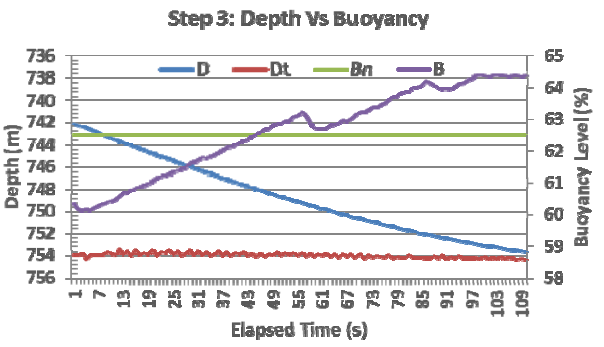

(b) Depth Vs Buoyancy

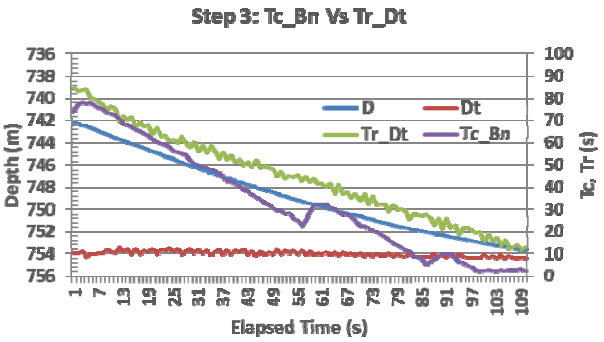

(c) T_c Vs T_r

Fig. 19 Altitude control: Step 3.

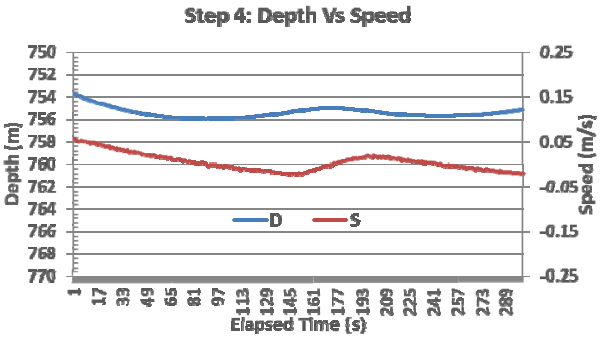

(a) Depth Vs Speed

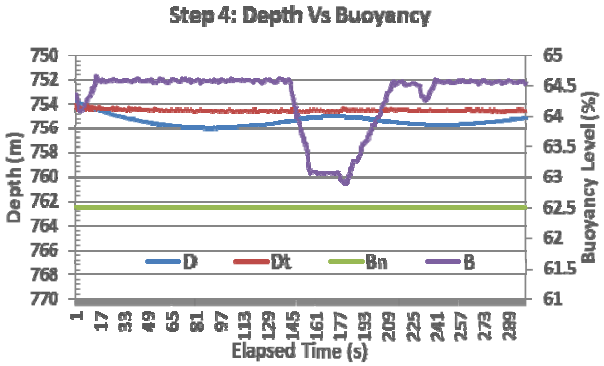

(b) Depth Vs Buoyancy

Fig. 20 Altitude control: Step 4.

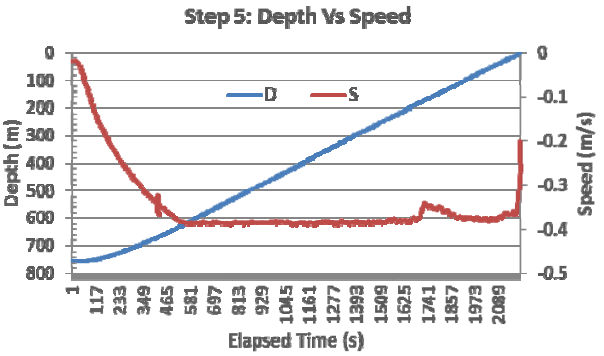

(a) Depth Vs Speed

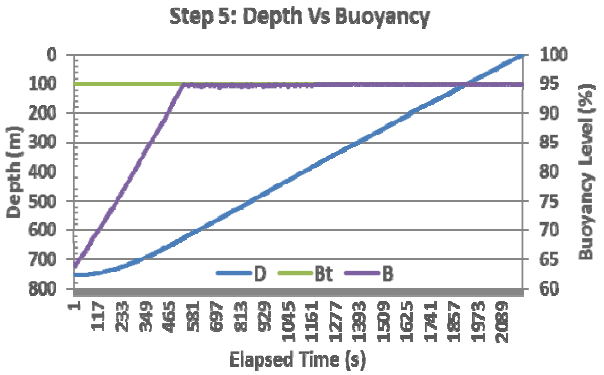

(b) Depth Vs Buoyancy

Fig. 21 Altitude control: Step 5.

In summary, the 3 stages of predictive depth control succeeded to bring the robot to the target altitude with a buoyancy value close to the neutral and with vertical speed almost equal to 0. Besides, the altitude stabilizer succeeded to maintain the robot within 1 m from the target altitude. The definition of the certain depth helped to reduce the time to reach the target altitude.

6. Conclusions

A new method for depth control using the buoyancy control device was developed. A model of the buoyancy variation with time was established. It was built based on the results obtained in high pressure tank experiment and several at-sea experiments. The depth control algorithm is based on the comparison between the time estimated for the robot to change its buoyancy from its current value to the neutral value, and the time expected for the robot to reach the target depth. The method was demonstrated at-sea experiments in Toyama Bay in Japan in March 2016. It showed the ability of the control algorithm to smoothly bring the robot to the target depth without a significant overshoot. The algorithm is characterized by its flexibility and does not require a strict determination neutral buoyancy value. A margin of inaccuracy can be customized before performing the dive. The method could be further adapted to perform an altitude control through a progressive depth control algorithm based on 4 steps. The experiment results showed that it worked properly.

Acknowledgements

This research project was funded for 2011FY-2015FY by Grant-in-Aid for Scientific Research(S) of Japan Society for the Promotion of Science (No. 23226017).

References

[1] Seymour, R. J., and Geyer, R. A. 1992. “Fates and Effects of Oil Spills.” *Annual Review of Energy and the Environment*: 261-83.

[2] Jakuba, M. V. et al. 2011. “Toward Automatic Classification of Chemical Sensor Data from Autonomous Underwater Vehicles.” *Intelligent Robots and Systems, IEEE/RSJ International Conference on Intelligent Robots and Systems*: 4722-7.

[3] Harvey, J. et al. 2012. “AUVs for Ecological Studies of Marine Plankton Communities.” *Sea Technology* 53 (9): 51.

[4] Roemmich, D. et al. 2009. “The Argo Program Observing the Global Ocean with Profiling Floats.” *Oceanography* 22 (2): 34-43. doi:10.5670/oceanog.2009.36.

[5] Eriksen, C. C. et al. 2001. “Seaglider: Along-Range Autonomous Underwater Vehicle for Oceanographic Research.” *IEEE Journal of Oceanic Engineering* 26 (4).

[6] Choyekh, M. et al. 2014. “Vertical Water Column Survey in the Gulf of Mexico Using Autonomous Underwater Vehicle SOTAB-I.” *Marine Technology Society Journal*: 88-101.

[7] Hallegraeff, G. 1998. “Transport of Toxic Dinoflagellates Via Ships’ Ballast Water: Bio-economic Risk Assessment and Efficacy of Possible Ballast Water Management Strategies.” *Marine Ecology Progress Series Mar. Ecol. Prog. Ser.* 168: 297-309. doi:10.3354/meps168297.

[8] Zhang, F., and Dickman, M. 1999. “Mid-ocean Exchange of Container Vessel Ballast Water. 1: Seasonal Factors Affecting the Transport of Harmful Diatoms and Dinoflagellates.” *Marine Ecology Progress Series Mar. Ecol. Prog. Ser.* 176: 243-51. doi:10.3354/meps176243.

[9] Clarke, M. R. 1978. “Physical Properties of Spermaceti Oil in the Sperm Whale.” *Journal of the Marine Biological Association of the United Kingdom J. Mar. Biol. Ass.* 58 (01): 19. doi:10.1017/s0025315400024383.

[10] Mcfarland, D., Gilhespy, I., and Honary, E. 2003. “DIVEBOT: A Diving Robot with a Whale-Like Buoyancy Mechanism.” *Robotica* 21 (4): 385-98. doi:10.1017/s026357470300496x.

[11] Shibuya, K., Kishimoto, Y., and Yoshi, S. 2013. “Depth Control of Underwater Robot with Metal Bellows Mechanism for Buoyancy Control Device Utilizing Phase Transition.” *Journal of Robotics and Mechatronics (JRM)* 25 (5): 795-803. doi:10.20965/jrm.2013.p0795.

[12] Bond, C. E. 1996. *Swim Bladder, Biology of Fishes* (2nd ed.). Orlando: Saunders College Publishing.

[13] Um, T. I., Chen, Z., and Bart-Smith, H. 2011. “A Novel Electroactive Polymer Buoyancy Control Device for Bio-Inspired Underwater Vehicles.” *2011 IEEE International Conference on Robotics and Automation*: 172-7. doi:10.1109/icra.2011.5980181.

[14] Barker, L. 2014. *Closed-Loop Buoyancy Control for a Coastal Profiling Float*. MBARI Intern Report.

[15] Izawa, K., Mizuno, K., Miyazaki, M., Inoue, A., Ando, K., Takatsuki, Y., Kobayashi, T., and Takeuchi, K. 2002. *On*

the Weight Adjustment of Profiling Floats. ARGO Technical Report FY2001, 18-35.

[16] Kato, N. et al. 2015. "Autonomous Spilled Oil and Gas Tracking Buoy System and Application to Marine Disaster Prevention System." Interspill 2015, Amsterdam, Netherland.